Asian Journal of Chemistry; Vol. 37, No. 8 (2025), 1927-1931

ASIAN JOURNAL OF CHEMISTRY

https://doi.org/10.14233/ajchem.2025.32894

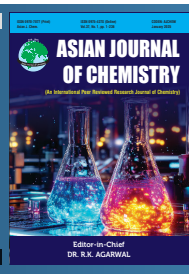


# Computational DFT Studies of CO Adsorption on Different 2D Materials

T. MD SAYEED[1,*], KAVIL JITHESH[2] and P.K. ANITHA[2]

[1]Department of Chemistry, Sir Syed College (Affliated to Kannur University), Taliparamba-670142, India
[2]Department of Chemistry, Sree Narayana College (Affliated to Kannur University), Kannur-670007, India

*Corresponding author: E-mail: sayeed@sirsyedcollege.ac.in

*Received*: 15 October 2024; *Accepted*: 5 July 2025; *Published online*: 31 July 2025; AJC-22071

Computational density functional theory (DFT) has been employed to predict the carbon monoxide (CO) adsorption on the surface of four studied different 2D materials like boron nitride, graphene, silicene and germanene. This study utilizes DFT calculations for graphene, two-dimensional hexagonal boron nitride, silicene, and germanene, along with their heterostructures with carbon monoxide. The stability of these materials has also been assessed. Adsorption energy is estimated and compared using self-consistent field calculations. The charge density distribution plot is thoroughly examined to confirm the bonding characteristics and electron delocalization in the relevant 2D material and adsorbed heterostructure. The findings from the calculation of CO adsorption energy revealed that graphene is a more effective adsorbate than boron nitride, whereas germanene demonstrates better performance than silicene, supported by consistent results from the adsorption energy analysis. The adsorption energy from self-consistent field energy calculations matches the charge distribution of two-dimensional materials after CO adsorption.

**Keywords: DFT, Graphene, Silicene, Boron nitride, Germanene, Adsorption energy, Electron density plot, Electron localization.**

## INTRODUCTION

Among the 2D materials, the extraordinary characteristics of graphene has sparked a surge of interest among researchers. Graphene is composed of layers of carbon atoms arranged in a hexagonal lattice. The single layer graphite has garnered attention for fundamental scientific exploration and its prospective uses. Graphene is anticipated to maintain a flawless flatness; however, the presence of ripples arises from thermal fluctuations [1]. The single layer graphene stands out as the optimal choice, while samples with two or more layers are also being explored with significant interest. Three distinct forms of graphene are identified: single layer graphene (SG), bilayer graphene (BG) and few-layer graphene (FG, with layers ≤ 10). The micromechanical cleavage of highly oriented pyrolytic graphite (HOPG), chemical vapor deposition (CVD) on the surfaces of single crystals of metals such as nickel and colloidal suspensions in selected solvents are among the techniques employed for the synthesis of single-layer graphene [2].

Silicene, the silicon counterpart of graphene, presents a significant challenge in the synthesis of one-atom-thick sheets due to the covalent characteristics of the interlayer Si-Si bond found in bulk silicon and the absence of a graphitic form of silicon. The enhanced spin orbit coupling of silicene presents promising opportunities for advancements in spintronic devices. The process of hydrogenation is more favourable in silicene, since it tends to favour $sp^3$ hybridization rather than $sp^2$. The silicene sheets and nanoribbons over various substrates like silver, diboride thin films and iridium have been reported [3]. Similarly, germanene, an analogue of graphene, but made of germanium atoms instead of carbon, is prepared by low temperature topochemical reaction of $CaGe_2$ with HCl [4,5]. Bianco *et al*. [6] reported that the exfoliation of GeH and studied some properties of germanene such as thermal stability and optical band gap. This analogue of graphene exhibits a direct band gap and its predicted charge carrier mobility >18000 $cm^2 v^{-1} s^{-1}$. It is five times higher than that of crystalline germanium [4].

In this work, the adsorption behaviour of CO on the surface of 2D materials like boron nitride, graphene, silicene and germanene through density functional theory (DFT) simulations is studied in order to investigate the most suitable heterostructure for CO adsorption by studying the adsorption energy, charge

TABLE-1
CALCULATED BOND PARAMETERS, FORCE ACTING ON THE ATOM, BOND ANGLE AFTER GEOMETRY OPTIMIZATION

| Slab structure | Total force acting on atoms (Ry) | Total SCF correction | Total pressure on atom (kbar) | Bond distance | Bond angle | Dihedral angle |
|---|---|---|---|---|---|---|
| Graphene | 0.000189 | 0.00001 | 0.02 | 1.4216 | 120 | 0 |
| Boron nitride | 0.000002 | 0.000027 | -0.01 | 1.4491 | 120 | 0 |
| Silicene | 0.003887 | 0.000017 | 0.84 | 2.2721 | 116.345 | 37.007 |
| Germanene | 0.000041 | 0.000087 | 1.55 | 2.4064 | 111.942 | 53.374 |

transfer, energy gap, electron density (ED) and electrostatic potential (ESP) maps. In order to gain a deeper understanding of the energy gap, we examined the density of states (DOS) and partial density of states (PDOS) spectra.

## COMPUTATIONAL METHODS

**Method of calculation:** The theoretical calculations for CO adsorption on selected 2D materials such as boron nitride, graphene, silicene and germanene were conducted using a plane-wave basis set and the projector augmented-wave method with the Quantum Espresso package, solving the Kohn-Sham equations [7]. The core electron and their interaction with valence electrons were described by ultrasoft pseudopotentials [8]. Exchange and correlation effects were taken into account *via* the generalized gradient approximation (GGA) and the Perdew-Burke-Ernzerhof (PBE) exchange and the correlation potential. To examine the surface properties, a two-layered supercell slab was utilized to expose the surface. A slab structure was built using a 2 × 2 × 2 supercell of boron nitride, graphene, silicene and germanene, and a CO molecule was placed 2 Å above the surface of each slab to study its adsorption behaviour. The wave function was expanded in a plane-wave basis with a kinetic energy cut-off of 80 Ry for boron nitride slab, 45Ry for germanene, 75 Ry for graphene and 80 for silicene. We use an energy cut off for the plane-wave basis set of 450 Ry for boron nitride, 600 Ry for graphene, 600 Ry for silicene and 500 Ry for germanene. The network which is converged includes the 4 × 4 × 2, 8 × 8 × 2, 5 × 5 × 2, and 5 × 5 × 2 Monkhorst-Pack (MP) grids, which are applied to the Brillouin zone of the unit cell of the appropriate slab structure. The atomic relaxations were observed to occur until the residual forces on the atoms were less than $10^{-4}$ and the total energies converged to within $10^{-4}$ eV.

In order to minimize slab-slab interactions, the supercell includes a 15 Å vacuum space above this surface. The valence electron density is obtained by self-consistent iterative diagonalization of the Hamiltonian, with Pulay mixing of the output and input densities by 40%. Target pressure [kbar] = 0.0 in a relaxation calculation and convergence threshold on the pressure is 0.5 kbar. All energies have been extrapolated to T = 0 K. Self-consistence field calculation energy are converged $10^{-9}$ and maximum step used is 80. Calculation was performed using scf calculation in the module. The bond length of CO and carbon distance from surface is fixed for all surfaces [9].

Calculation of the cohesive energy for all four two dimensional structure was obtained as the total energy per formula unit minus the total energy of a formula unit of free atoms [10]. From cohesive energy calculation we can predict the nature of bonding in these two dimensional material structure.

**CO adsorption energy:** The adsorption of CO molecules in the surface of each slabs are modelled so that it will generate the adsorption energy of CO in each of the surfaces. The position of CO in all of the surface was set to be directly above the outermost atom, as it known to be the active site of the adsorption. The distance of the CO molecules to the outermost metal atoms was set to be 2 Å. Average adsorption energies, $E_{ads}$, have been calculated according to the following equation [11]:

$$-E_{ads} = E_{slab-CO} - E_{slab} - E_{CO}$$

where $E_{ads}$ is defined so that the positive adsorption energies correspond to the stable surface binding.

## RESULTS AND DISCUSSION

**Geometry optimization:** A carbon-carbon bond distance of 1.42646 Å bond angle of 120º is displayed in the optimized graphene structure and both the width and the height of the unit cell are 4.9244 Å. Along the *z*-axis, a vacuum of 15 Å is introduced. Table-1 displays the additional details following geometry optimization.

In optimized geometry of silicene, unit cell has two Si atoms. The vertical distance between two Si atoms at sites had a low buckled minimum energy structure with a lattice constant of 3.903 Å. The bond angle in silicene lies between the hybridized structures of $sp^3$ (109.47º) and $sp^2$ (120º), which exhibit that the hybridization in silicene is a combination of $sp^2$ and $sp^3$. The reason for the buckling observed in silicene is the weak π-π bond between Si atoms, as the Si-Si distance is significantly greater than that of graphene (C-C = 1.42º). The binding energy of a system increases due to buckling by increasing the overlap between π and σ orbitals. The presence of buckling can be explained on the basis of the Jahn-Teller distortion [12].

The stress tensor was derived using the Broyden-Fletcher-Goldfarb-Shanno (BFGS) technique, resulting in the optimal relaxed coordinates. The stress tensor derived from the calculations is shown in Table-2. The xx and yy stress tensor components diverge from the zz stress tensor component, indicating that a non-isotropic stress is necessary to achieve the specified volume and shape of the unit cell. Following this optimization,

TABLE-2
STRESS TENSOR AND PRESSURE (CARTESIAN AXIS) CALCULATED FOR RELAXED STRUCTURE USING BFGS ALGORITHM

| | Computing stress (Cartesian axis) (Ry per bohr$^3$) | | Pressure (kbar) |
|---|---|---|---|
| | XX or YY | ZZ | |
| Graphene | 0.00000037 | -0.00000040 | 0.02 |
| Boron nitride | -0.00003498 | -0.00000070 | -0.01 |
| Silicene | 0.00000821 | 0.00000067 | 0.84 |
| Germanene | 0.00002095 | -0.00001037 | 1.55 |

all diagonal components of the stress tensor converge to identical values, representing hydrostatic pressure that is uniform in all directions within $10^{-4}$ [13].

**Cohesive energy:** The calculated cohesive energy in electron volt is shown in Table-3. The stability of boron nitride structure showed more stable than graphene. The same observation is reported in the literature from the experimental result [10]. It is also indicated that germanene is least stable among these structures.

**CO adsorption energy:** The average adsorption energies per unit cell were calculated for graphene-CO, BN-CO, silicene-CO and germanene-CO are listed in Table-4. The differences in the adsorption energy between the slabs and hetrostructure are very small. The adsorption values for BN-CO and graphene–CO are comparable, as are those for Ge-CO and Si-CO, measuring 0.076338 Ry and 0.023172 Ry, respectively. Graphene exhibits the superior adsorption properties compared to 2D BN, with an adsorption energy of 0.2322 Ry for graphene and 0.212331 Ry for BN, whereas germanene has superior CO adsorption compared to silicene. The adsorption energy for germanene is 0.076338 Ry, while for silicene it is 0.023172 Ry.

**Electron density plot:** A two-dimensional contour plot of electron density has been generated using the post-processing tool of Quantum Espresso. Electron density of bond is plotted to compare electron density between the bonds of slab structure. Electron delocalization in the BN bond is absent in a 2D boron nitride slab (Fig. 1), but in graphene (Fig. 2), there is extensive delocalization (red), which is also visible in the C-C bond and indicates that the charges are uniformly distributed among the bonds.The delocalization in silicene is substantially inferior to that in graphene, and there is an absence of electron density between Ge-Ge bonds in germanene. Additionally, it is evident that there is no electron delocalization in the Ge-Ge bond.

We established a CO adsorbed configuration for these four slab structures and illustrated the electron density between the slab-CO bonds. The outcome is illustrated in Fig. 3 and the significant delocalization is evident only in graphene. The optimized structure of silicene and germanene is not flat and the CO is positioned with an identical bond distance relative to all two-dimensional materials. Significant charge density is observed in the boron-carbon bond within the BN-CO structure, while a delocalized and uniform charge distribution is present in the graphene-CO bond. The silicene-CO structure demonstrates that the electron density of carbon is polarized towards silicon within the silicene framework. The germanene structure exhibits a reduced charge delocalization in the Ge-Ge bond, alongside significant bonding in the Ge-CO bond, which is superior to that of the Si-CO bond and a 2D charge density contour plots are shown in Fig. 4. Based on this, a significant charge density present between the boron-carbon bond of BN-CO, alongside a delocalized and uniform charge distribution in the graphene-CO bond. The structure of silicene-CO reveals that the electron density of carbon is polarized towards silicon within the silicene framework. The germanene structure exhibits

TABLE-3
COHESIVE ENERGY CALCULATED (ELECTRON VOLT) FOR 2D MATERIAL

| 2D Structure | Cohesive energy (eV) | Fermi energy (eV) | HOMO (eV) | LUMO (eV) |
|---|---|---|---|---|
| Boron nitride | 0.87373595 | 0.7214 | -0.7955 | 4.1892 |
| Graphene | 0.84709356 | -2.7817 | -2.9649 | -1.7286 |
| Silicene | 0.39740067 | -3.1454 | -4.6733 | -3.3012 |
| Germanene | 0.3131913 | -2.6360 | -2.7918 | -2.0005 |

TABLE-4
ADSORPTION ENERGY CALCULATED FROM SCF CALCULATION

| Slab structure | Slab energy (Ry) | Calculation accuracy (<) | Slab-CO energy (Ry) | Calculation accuracy | Adsorption energy in Rydberg (Ry) |
|---|---|---|---|---|---|
| Graphene | -91.16486010 | $6.1 \times 10^{-9}$ | -134.12819497 | $1.1 \times 10^{-10}$ | 0.232247 |
| Boron Nitride | -105.33680633 | $1.4 \times 10^{-9}$ | -148.32005750 | $1.4 \times 10^{-9}$ | 0.212331 |
| Silicene | -90.98397746 | $4.6 \times 10^{-10}$ | -134.15638774 | $7.7 \times 10^{-10}$ | 0.023172 |
| Germanene | -1690.96211047 | $6.3 \times 10^{-10}$ | -1734.09601480 | $4.5 \times 10^{-10}$ | 0.076338 |

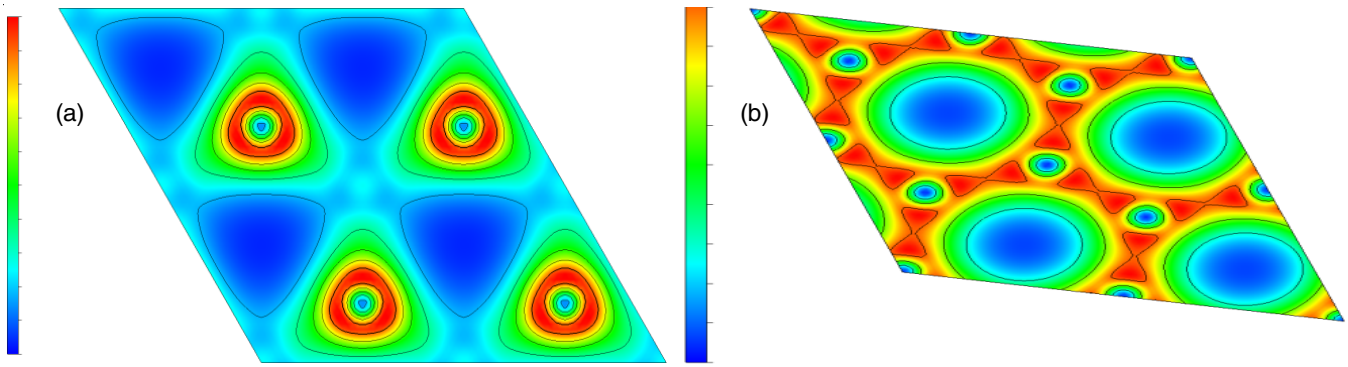


Fig. 1. 2 Dimensional plot of charge density 2D BN slab (a) and charge density graphene slab (b)

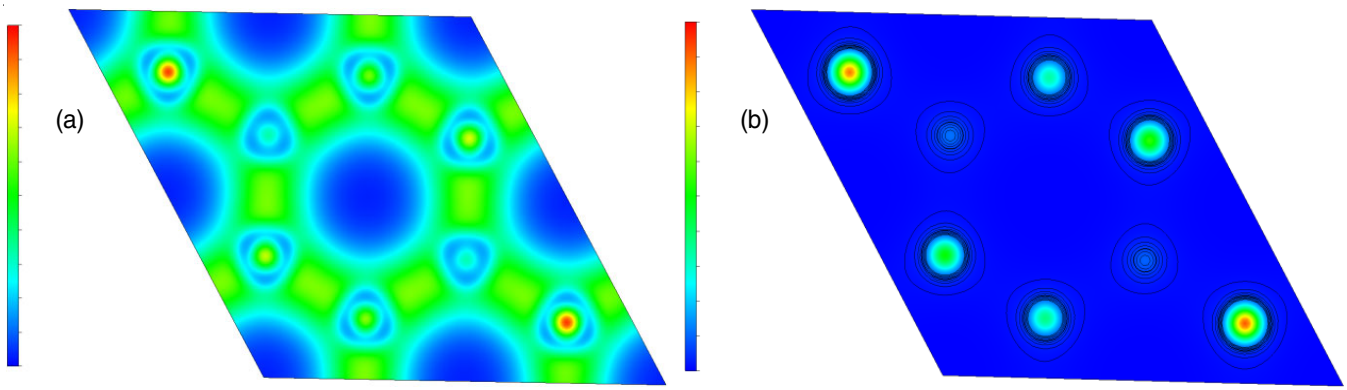


Fig. 2. 2 Dimensional plot of charge density 2D silicene slab (a) and charge density germanene slab (b)

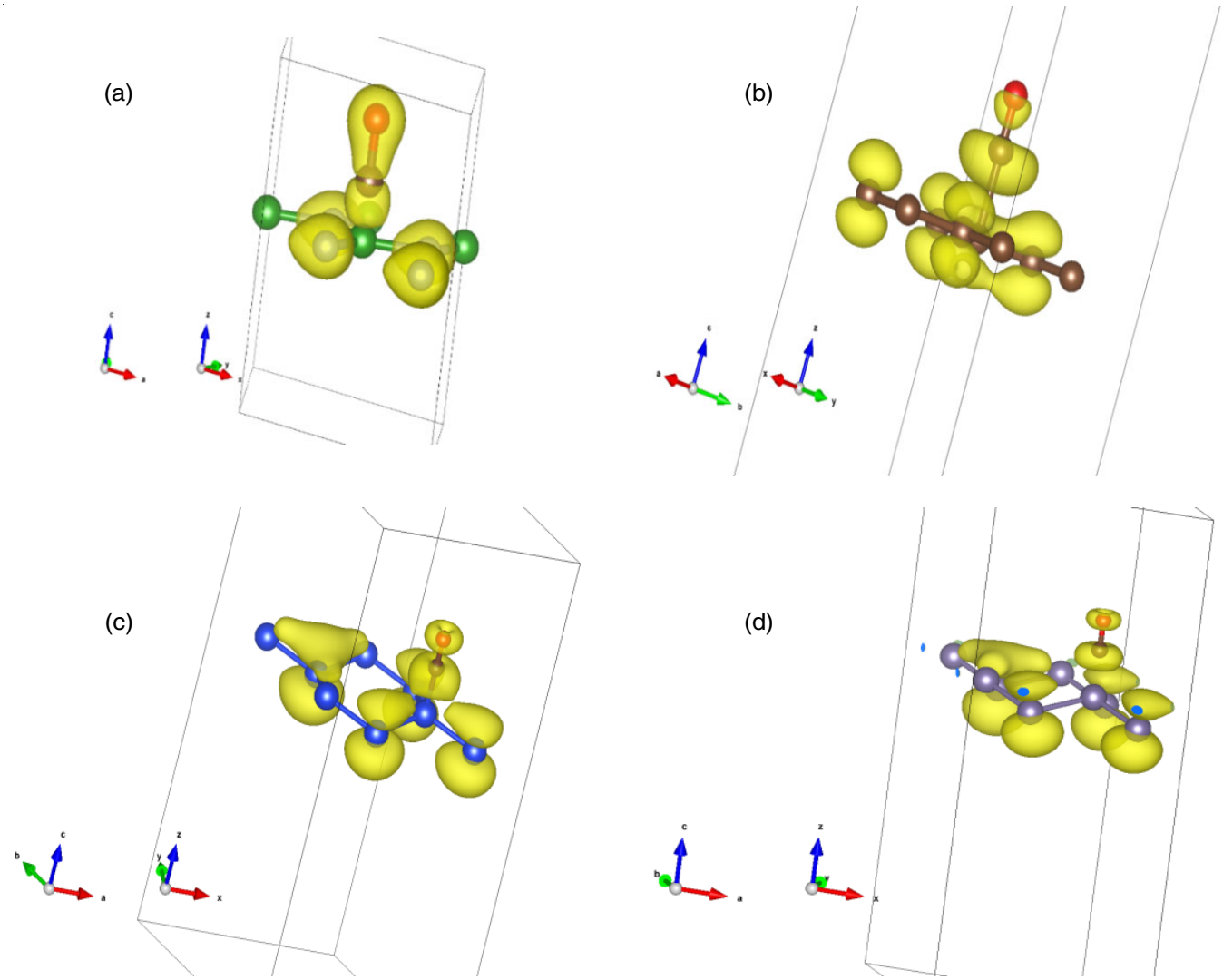


Fig. 3. Electron density plot for boron nitride-CO (a), graphene-CO (b) silicene-CO (c) and germanene-CO (d)

reduced the charge delocalization in the Ge-Ge bond, while demonstrating significant bonding in the Ge-CO bond.

## Conclusion

DFT computations of two-dimensional materials, including boron nitride, graphene, silicene, and germanene, regarding CO adsorption and their respective adsorbed structures have yielded promising results. The obtained results are used to predict the stability and nature of bonding and potential application in various fields. The optimized structures of silicene and germanene possess a planar configuration similar to that of graphene and boron nitride. The calculation of cohesive energy indicates that boron nitride exhibits greater stability compared to graphene whereas germanene exhibits the least stability. The results of

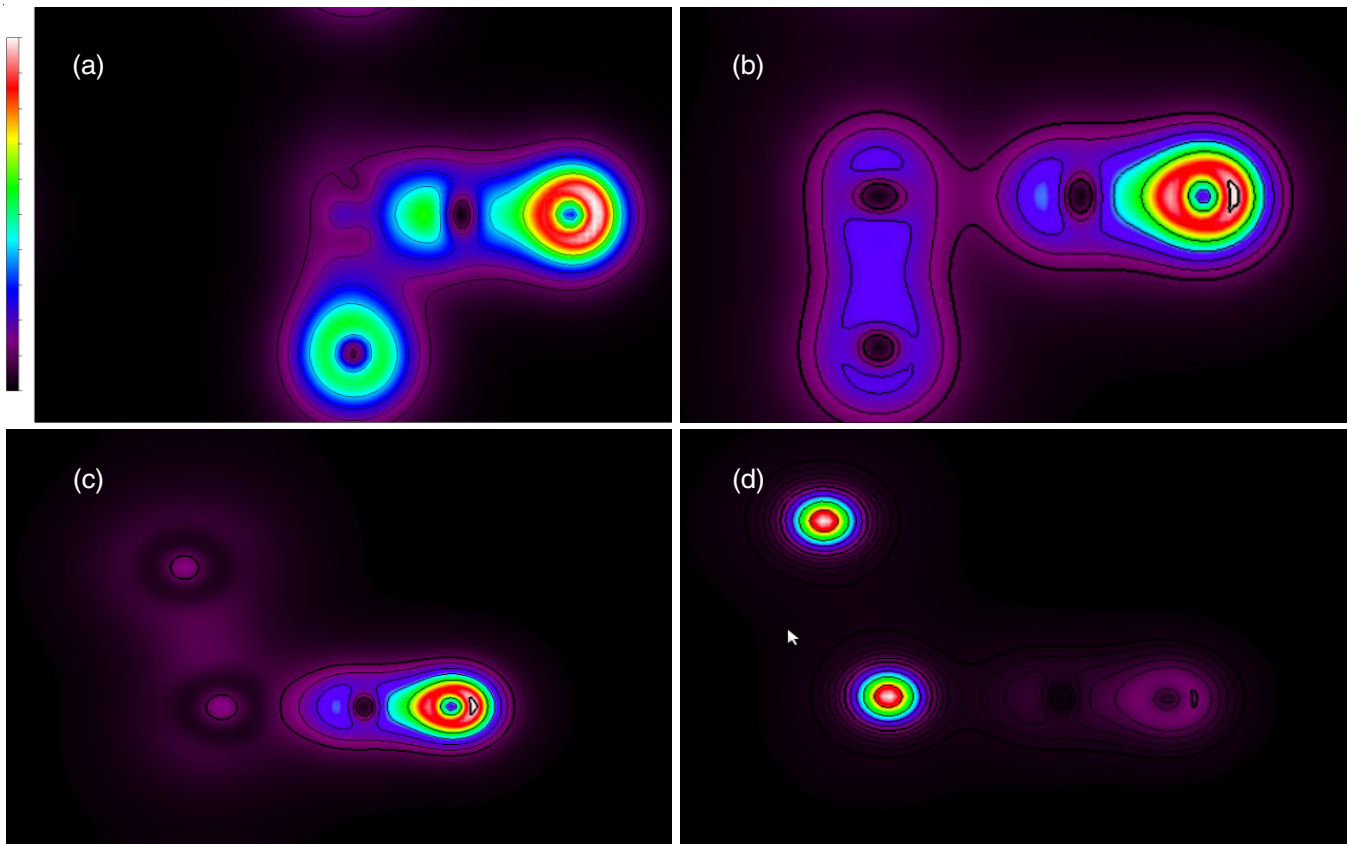


Fig. 4. (a) Boron nitride-CO, (b) graphene-CO, (c) Si-CO and (d) Ge-CO bond electron density plot

the CO adsorption energy calculation highlight that graphene serves as a superior adsorbate compared to boron nitride, while germanene outperforms silicene, with consistent findings from the adsorption energy analysis. The plotted charge density distribution reveals crucial insights into bonding and electron localization within these structures. Graphene exhibits significant levels of delocalization, while a substantial electron density delocalization is also visible in silicene. For germanene, there is no evidence of electron delocalization; however, the adsorption of CO is more favourable. The electron density distribution plot indicates that the M-CO bond in germanene exhibits superior electron density compared to silicene, a finding that is also supported by the adsorption energy calculations. The impact of CO adsorption on the charge distribution of studied 2D materials aligns well with the adsorption energy derived from self-consistent field energy calculations.

## ACKNOWLEDGEMENTS

The authors thank Ajit Balakrishnan foundation for establishing the Computational Chemistry laboratory at Sir Syed College, Taliparamba, India.

## CONFLICT OF INTEREST

The authors declare that there is no conflict of interests regarding the publication of this article.

## REFERENCES

1. C.N.R. Rao, A.K. Sood, K.S. Subrahmanyam and A. Govindaraj, *Angew. Chem. Int. Ed. Engl.*, **48**, 7752 (2009); https://doi.org/10.1002/anie.200901678
2. S. Hofmann, P. Braeuninger-Weimer and R.S. Weatherup, *J. Phys. Chem. Lett.*, **6**, 2714 (2015); https://doi.org/10.1021/acs.jpclett.5b01052
3. D. Jose and A. Datta, *Acc. Chem. Res.*, **47**, 593 (2014); https://doi.org/10.1021/ar400180e
4. T. Giousis, G. Potsi, A. Kouloumpis, K. Spyrou, Y. Georgantas, N. Chalmpes, K. Dimos, M.-K. Antoniou, H.J. Kim, G. Papavassiliou, A.B. Bourlinos, H.J. Kim, V.K.S. Wadi, S. Alhassan, M. Ahmadi, B.J. Kooi, G. Blake, D.M Balazs, M.A. Loi, D. Gournis and P. Rudolf, *Angew. Chem. Int. Ed. Engl.*, **60**, 360 (2020); https://doi.org/10.1002/anie.202010404
5. A. Molle, J. Yuhara, Y. Yamada-Takamura and Z. Sofer, *Chem. Soc. Rev.*, **54**, 1845 (2025); https://doi.org/10.1039/D4CS00999A
6. E. Bianco, S. Butler, S.Jiang, O.D. Restrepo, W. Windl and J.E. Goldberger, *ACS Nano*, **7**, 4414 (2013); https://doi.org/10.1021/nn4009406
7. W. Kohn and L.J. Sham, *Phys. Rev.*, **140(4A)**, A1133 (1965); https://doi.org/10.1103/PhysRev.140.A1133
8. P. Giannozzi, O. Baseggio, P. Bonfà, D. Brunato, R. Car, I. Carnimeo, C. Cavazzoni, S. de Gironcoli, P. Delugas, F. Ferrari Ruffino, A. Ferretti, N. Marzari, I. Timrov, A. Urru and S. Baroni, *J. Chem. Phys.*, **152**, 154105 (2020); https://doi.org/10.1063/5.0005082
9. I, Kurnia, P, Siahaan and A, Suseno, *IOP Conf. Ser.: Mater. Sci. Eng.*, **959**, 012004 (2020); https://doi.org/10.1088/1757-899X/959/1/012004
10. C. Kamal, *arXiv*, **1202**, 2636 (2012); https://doi.org/10.48550/arXiv.1202.2636
11. A.R. Soltani and M.T. Baei, *Computation*, **7**, 61 (2019); https://doi.org/10.3390/computation7040061
12. B. Feng, Z. Ding, S. Meng, Y. Yao, X. He, P. Cheng, L. Chen and K. Wu, *Nano Lett.*, **12**, 3507 (2012); https://doi.org/10.1021/nl301047g
13. https://www.quantum-espresso.org/documentation/input-data-description/